Data-driven interferometry method to remove spatially aliased and non-linear surface waves

Corentin Chiffot[1], Anthony Prescott[1], Martin Grimshaw[1], Francesca Oggioni[1], Monika Kowalczyk-Kedzierska[1], Sharon Cooper[1], Rodney G. Johnston[2] and David Le Meur[1], [1]CGG, [2]BP*

Summary

We propose a data-driven interferometry technique to remove low frequency aliased and non-conical surface waves in cross-spread domain. Despite insufficient sampling of the constructive regions in the cross-spread domain, the proposed approach has been designed for effective handling of any kind of 3D geometry from Narrow to Wide-Azimuth land data using prior regularization and/or densification. This implementation provides a cost-effective workflow for large datasets and produces good removal of spatially aliased non-linear surface waves with minimal primary leakage.

Introduction

Land seismic data contains energetic surface waves, which may be isolated and inverted to characterize the near surface. However it is still necessary to remove them before processing the reflected body waves. The most energetic surface waves are the low frequency dispersive Rayleigh waves propagating along the free surface. This ground-roll is usually removed by filtering in a transformed domain (such as frequency-wavenumber, S domain, empirical mode decomposition) (Askari and Siahkoohi, 2007; Dong et al., 2013), or by subtracting a noise model constructed with parameters extracted from the transformed signal in the f-x domain (Le Meur et al., 2008). However, when the acquisition geometry is insufficiently sampled, it causes spatial aliasing on the recorded surface waves that can make the application of these methods challenging. Furthermore we can face a complex near-surface overburden which distorts the wave fronts (showing non-conical arrivals), or acquisition designs where source or receiver lines are not acquired in a strictly orthogonal manner (like serpentine, zig-zag or checkerboard acquisitions for instance).

During the last decade, interferometric methods have been developed to provide new data-driven approaches as, for example, the surface-wave estimation. If sources and receivers are located on the free surface, stacking cross-correlations between traces of source gathers can retrieve the surface wave Green's function between two receivers, due to the fact that the body waves are under-estimated in the process (Dong et al., 2006; Forghani and Snieder, 2010). Those techniques have been extended to extract the surface waves between a source and a receiver (Duguid et al., 2011). Additionally, it has been shown that prior separation of incident and scattered surface waves allows creation of interferometric models of both incident surface waves and scattered surface waves (Halliday et al., 2010; Guo et al., 2015). Similarly, prior separation of the different surface wave modes gives better separate models (Halliday and Curtis, 2008).

In this paper, we demonstrate the use of a data-driven interferometry approach in the cross-spread domain and its strength to model low frequency aliased and non-linear incident surface waves on 3D Wide-Azimuth land data.

Method

To estimate the surface wave's model, we use the approximation of source-receiver Green's function in the frequency domain defined by the trilinear operator (Curtis and Halliday, 2010; Duguid et al., 2011), assuming Sommerfeld radiation conditions:

$$G(x_2,x_1)+G^*(x_2,x_1) \approx C\int_{x\in S}\int_{x'\in S'} G(x',x_1)G^*(x',x)G(x_2,x)dS'dS \quad (1)$$

where $G(x_2,x_1)$ is the Green's function recorded at x_2 for an impulsive source at x_1, the star denotes complex conjugation, S is a boundary of sources, S' is a boundary of receivers, C is a frequency dependent scaling factor. S may enclose x_2 but not x_1, and S' encloses both; alternatively S may enclose both, and S' only x_1 (Curtis and Halliday, 2010; Duguid et al., 2011). As a continuous boundary of sources or receivers is not available in practice, we sample the constructive regions of the integrals with the available survey sources and receivers as described by Halliday et al. (2010):

$$G(x_2,x_1)+G^*(x_2,x_1) \approx C\sum_{x\in S,x'\in S'} G(x',x_1)G^*(x',x)G(x_2,x) \quad (2)$$

In our case of free surface sources and receivers, the estimate of the Green's function is dominated by surface waves (Dong et al., 2006; Forghani and Snieder, 2010; Curtis and Halliday, 2010). A similar practical form is also used by An and Hu (2016), using surface wave estimates instead of recorded Green's functions and deconvolving the terms of the sum in order to reduce the wavelet distortion introduced by the source amplitude spectrum present in each factor of the terms. The scaling factor C can also be recovered during a later adaptive subtraction of the model.

This approximation is computed for each source-receiver pair (Figure 1c) of Normal Move-Out (NMO) corrected cross-spread data (Figure 1a). The processing is applied separately on each cross-spread to avoid merging and to reduce computational memory, so only one source line and one receiver line are available for sampling the constructive regions of the integrals. By doing so, we expect a poor sampling of these regions. To further enhance the computation time, we restrict the available sources and receivers within an aperture radius centered around x_2 and x_1 (Figure 1c). In addition to using this surface wave estimate computed by a correlational and a convolutional interferometric integral, we also compute and add another surface wave estimate with two correlational integrals with both boundaries enclosing both x_2 and x_1, as presented by Curtis and Halliday (2010). Looking at the result we observe that the kinematic of the low frequency part of the non-conical surface waves has been well captured but not the aliased part (Figure 1a and 1d, see black dashed circles). Indeed, the poor sampling of the constructive regions violates the theoretical requirements of interferometry and that implies possibly incorrect amplitudes and phases estimation compared to the input data (Loer et al., 2013).

In order to correctly model the aliased part of the non-conical surface waves at the original coordinates, we used a multi-dimensional reversible irregular to regular mapping algorithm in the cross-spread domain (Poole, 2010; Sternfels et al., 2016). The densification factor in source and receiver lines is chosen so that surface waves are de-aliased before being modeled with our data-driven interferometry (Figures 2a and 2b). The use of the latter on regularized and densified cross-spreads allows the spatial aliasing (see black arrow), the amplitude and phase variation to be better taken into account and improves the kinematics of the non-linear shape of the ground-roll at broadside cable (Figure 2c and 2d, black circle and arrow). On this example, the higher the cross-spread density, the more accurate are the kinematics, amplitude and phase of the modeling, as expected by the finer sampling of the constructive regions of the interferometric integral.

Data example

We apply our data-driven interferometry approach on a 3D Wide-Azimuth survey from Oman acquired by BP (Bouska, 2009) that contains strongly aliased low frequency non-conical surface waves (Figures 3a and 3b). The latter were produced by a heterogeneous near-surface, an original acquisition design (serpentine receiver lines) with a 100 x 50m source/receiver spacing.

By applying the complete workflow described in the section above, regularization and densification are performed to obtain denser cross-spreads with 25 x 25m source/receiver spacing. Then, the data-driven interferometry method is applied on the densified cross-spreads with an aperture radius of 100m. The resulting model is mapped back to the original source/receiver positions (100 x 50m source/receiver spacing) and locally adaptively subtracted to the input data (Figures 3c and 3d). The output NMO-corrected Common Mid-Points show that from the nearest to the farthest offsets the low-frequency aliased non-conical surface waves have been removed without harming the weak primaries underneath, as shown by the black dashed circle and the red arrows (Figures 3a to 3d).

The results on stack sections confirm the benefit of such a method on this 3D Wide-Azimuth survey. The stack section of the input data (Figure 4a) is corrupted with strong amplitude apexes of surface waves and curtains of aliased surface waves. The difference (Figure 4c) shows that strong surface wave undulations through the section due to the complex heterogeneous near surface and the footprint of the serpentine acquisition have been well estimated. On the output data (Figure 4b), the amplitude of the primary events has been preserved throughout the section. The aliased low-frequency part of the ground-roll noise has been removed with minimal primary leakage damage.

Conclusion

We have applied our data-driven interferometry approach to model the surface waves on a 3D Wide-Azimuth land dataset with a complex near-surface and original acquisition design. Interferometry is performed with a prior regularization and/or densification in cross-spread domain in order to provide a cost-effective workflow. The proposed method has been able to produce good removal of low frequency aliased non-linear surface waves with minimal primary leakage.

Acknowledgments

The authors would like to thank BP Oman, the Ministry of Oil & Gas of the Sultanate of Oman, and CGG for their permission to publish this paper. We acknowledge the work of our colleagues of the CGG Crawley land subsurface imaging team.

Data-driven interferometry method to remove spatially aliased and non-linear surface waves

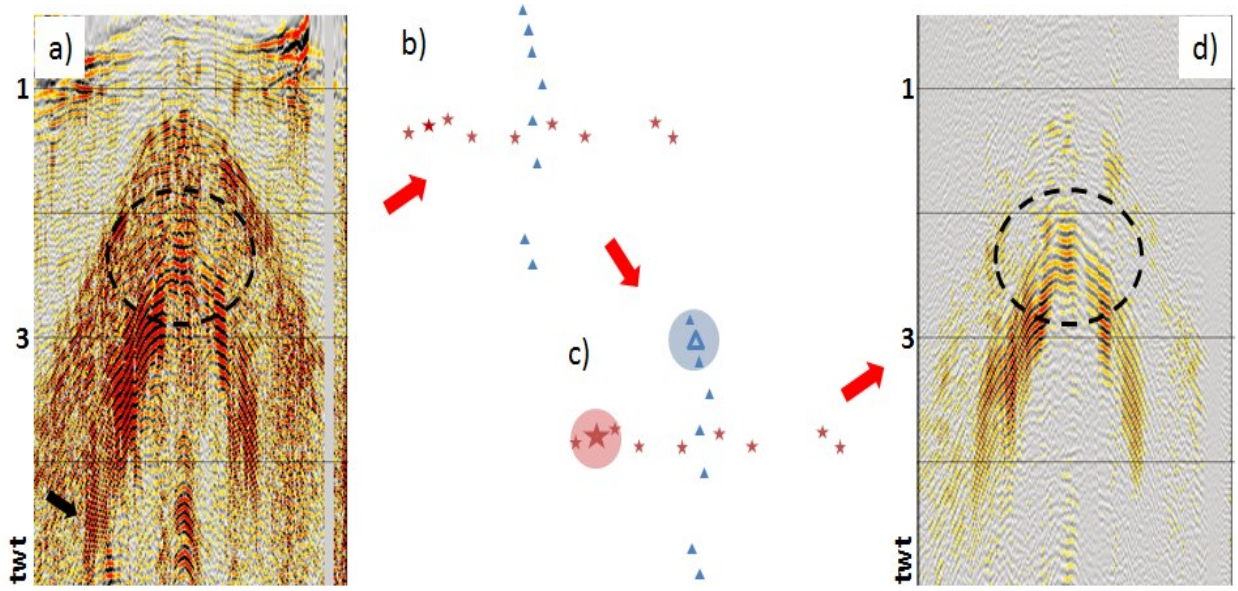

Figure 1: *(a) NMO corrected input data from an insufficiently sampled cross-spread with missing shots and receivers, (b) example configuration of a cross-spread, (c) restricted apertures (red and blue circles) are used to estimate the surface waves between hollow-star source and hollow-triangle receiver, (d) result of the data-driven interferometry applied on the input data (a). Stars depict sources and triangles depict receivers.*

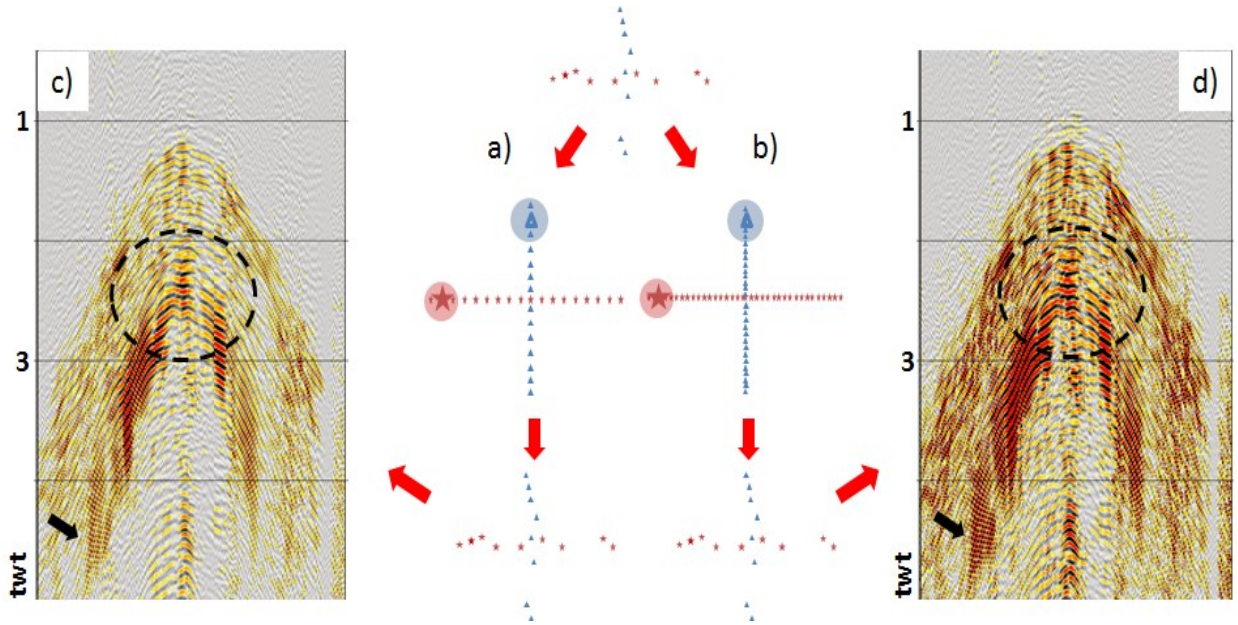

Figure 2: *(a) and (b) results after the regularization and densification by factors 2 and 4 respectively, prior to the data-driven interferometry, then mapped back to the original coordinates. For both (a) and (b) restricted apertures (red and blue disks) are used to estimate the surface waves between hollow-star source and hollow-triangle receiver. (c) and (d) panels are the results of the data-driven interferometry applied on input data of Figure 1a, on top of regularization/densification (a) and (b). Stars depict sources and triangles depict receivers.*

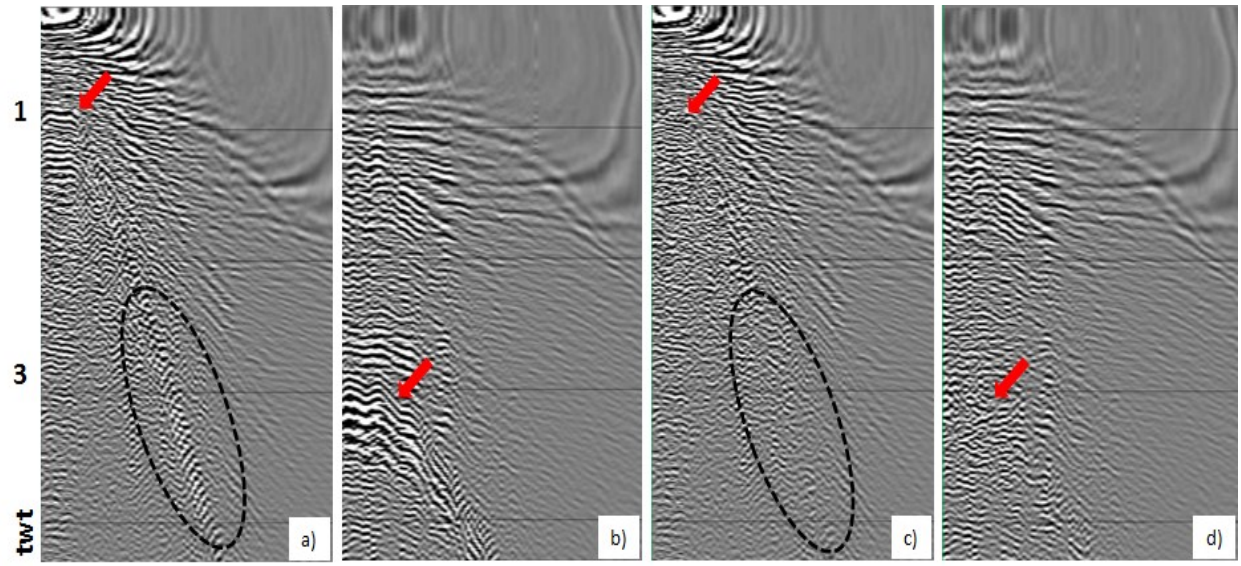

Figure 3: *NMO-corrected Common Mid-Points: (a) near and (b) broadside input data, (c) near and (d) broadside output data where the surface waves are modelled by our data-driven interferometry on top of a reversible regularization/densification followed by a local adaptive subtraction. Low frequency aliased non-conical surface waves have been efficiently removed*

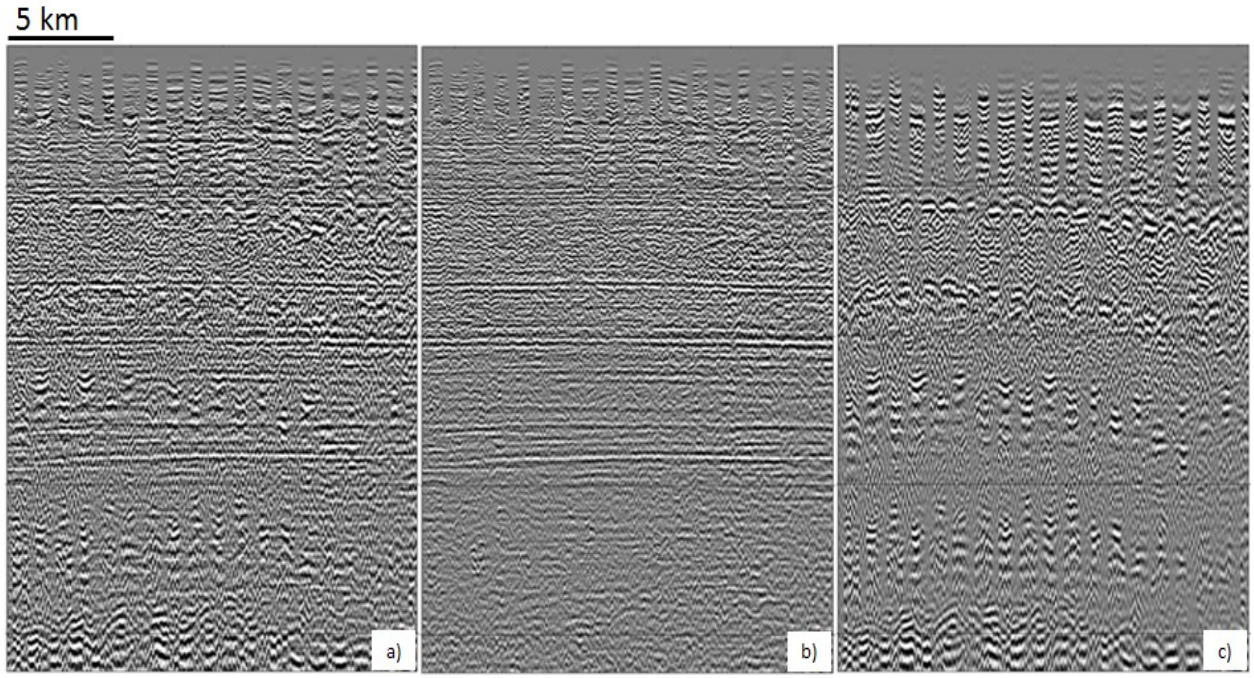

Figure 4: *Stack sections: (a) input data (b) output data where the surface waves are modelled by our data-driven interferometry on top of a reversible regularization/densification followed by a local adaptive subtraction (c) difference between (a) and (b).*